
Article:
Grayson, A., Hearnden, V.L. orcid.org/0000-0003-0838-7783, Bolt, R. et al. (3 more authors) (2018) Use of a Rho kinase inhibitor to increase human tonsil keratinocyte longevity for three-dimensional, tissue engineered tonsil epithelium equivalents. Journal of Tissue Engineering and Regenerative Medicine. ISSN 1932-6254

https://doi.org/10.1002/term.2590

Use of a Rho kinase inhibitor to increase human tonsil keratinocyte longevity for three-dimensional, tissue engineered tonsil epithelium equivalents

Amy K. Grayson[1], Vanessa Hearnden[2*], Robert Bolt[1], Ala Jebreel[3],

Helen E. Colley[1], Craig Murdoch[1]

[1]School of Clinical Dentistry, Claremont Crescent, University of Sheffield, S10 2TA, UK

[2] Department of Materials Science and Engineering, University of Sheffield, S3 7HQ, UK

[3] Sheffield Teaching Hospitals NHS Foundation Trust, Royal Hallamshire Hospital, Glossop Road, Sheffield, S10 2JF, UK

*Corresponding author:

Dr Vanessa Hearnden, Department of Materials Science and Engineering, University of Sheffield, Sheffield, S3 7HQ. UK.

Email: v.hearnden@sheffield.ac.uk

Short title: Y-27632 increases longevity of tonsillar keratinocytes to produce 3D tonsil equivalents.

Keywords: Y-27632, *Streptococcus pyogenes*, tissue engineering, tonsil, epithelium, keratinocytes, oropharynx.

Abstract

The generation of tissue-engineered epithelial models is often hampered by the limited proliferative capacity of primary epithelial cells. This study aimed to isolate normal tonsillar keratinocytes (NTK) from human tonsils, increase the lifespan of these cells using the Rho kinase inhibitor Y-27632 and to develop tissue-engineered equivalents of healthy and infected tonsil epithelium. The proliferation rate of isolated NTK and expression of c-MYC and p16INK4A were measured in the absence or presence of the inhibitor. Y-27632-treated NTK were used to generate tissue-engineered tonsil epithelium equivalents using de-epithelialized dermis that were then incubated with *Streptococcus pyogenes* to model bacterial tonsillitis, and the expression of pro-inflammatory cytokines was measured by cytokine array and ELISA. NTK cultured in the absence of Y-27632 rapidly senesced whereas cells cultured in the presence of this inhibitor proliferated for over 30 population doublings without changing their phenotype. Y-27632-treated NTK produced a multi-layered differentiated epithelium that histologically resembled normal tonsillar surface epithelium and responded to *S. pyogenes* infection by increased expression of pro-inflammatory cytokines including CXCL5 and IL-6. NTK can be isolated and successfully cultured *in vitro* with Y-27632 leading to a markedly prolonged lifespan without any deleterious consequences to the cell morphology. This functional tissue-engineered equivalent of tonsil epithelium will provide a valuable tool for studying tonsil biology and host-pathogen interactions in a more physiologically relevant manner.

1 Introduction

Located within the oropharynx, the human palatine tonsils are a component of Waldeyer's tonsillar ring; a series of immunocompetent lymphoid tissues whose function is to antigenically sample potentially infectious agents entering the aerodigestive tract. On their pharyngeal aspect, the palatine tonsils are covered by a stratified squamous epithelium that, although designed for protection, is highly susceptible to both viral and bacterial infections, including human papillomavirus (HPV) (Syrjanen, 2004), Epstein-Barr virus (EBV) (Pegtel*, et al.*, 2004) and Group A streptococcal infection (Wilkening and Federle, 2017).

Interrogation of the mechanisms by which pathogens bind to and invade tonsillar epithelium has been hampered by the absence of tonsillar tissue in small rodent models, rendering *in vivo* analysis impractical. This has lead researchers to develop alternative strategies to investigate host-pathogen interactions such as the use of isolated tonsillar cells (Turner*, et al.*, 2012) or *ex vivo* tonsillar explant tissue. Tonsillar explants consist of small sections of tonsillar tissue cultured immediately after excision and several groups have co-cultured these with various strains of *S. pyogenes* in an attempt to model the initial stages of tonsillar infection (Abbot*, et al.*, 2007, Bell*, et al.*, 2012, Smith*, et al.*, 2010). However, such explants have limited culture lifespan and are associated with significant variation in behaviour as a result of heterogeneous donor tissue. Tonsil explants are also logistically challenging, and require a regular supply of patient material in the face of reduced commissioning of tonsillectomy surgeries by health care providers. Other groups have used monolayer keratinocyte cultures to model tonsillar

infection (Ajello*, et al.*, 2002, Lace*, et al.*, 2009a). However, cells cultured in 2D do not exhibit the structural complexity of native tissue with respect to cell-cell interactions, paracrine signalling, morphogenesis, proliferation and differentiation and therefore represent poor models of stratified squamous epithelium (Moharamzadeh*, et al.*, 2012).

The limitations of monolayer culture have prompted interest in the use of tissue-engineered 3D models of squamous epithelium in order to study the mechanisms of infection. Recently, progress has been made in generating tissue-engineered tonsil epithelium. Kang *et al* developed a 3D *in vitro* infection model based on isolated human tonsillar keratinocytes cultured on a collagen matrix populated with murine 3T3 fibroblasts to examine HPV-mediated epithelial transformation (Kang*, et al.*, 2015); a similar model was also used by Temple and colleagues to monitor EBV-mediated epithelial infection (Temple*, et al.*, 2014). Although these *in vitro* models displayed a stratified epithelium, it is now clear that fibroblasts in the underlying connective tissue have a profound influence on the differentiation and keratinisation status of the epithelium (Mah*, et al.*, 2014), highlighting the importance of using anatomically matched fibroblasts (Sriram*, et al.*, 2015).

Another confounding factor in generating realistic *in vitro* epithelial equivalents is the limited lifespan of primary cultured keratinocytes and their rapid cellular senescence when cultured *in vitro* (Lundberg*, et al.*, 2000). Several strategies have been utilised to overcome this problem including immortalisation through transfection with viral oncogenes (Lace*, et al.*, 2009b, Spanos*, et al.*, 2008a) and stable elevated expression of hTERT (Dickson*, et al.*, 2000, Ramirez*, et al.*, 2001, Reijnders*, et al.*, 2015). Although

these immortalisation techniques have the distinct advantage of increasing the longevity of cells they also carry several disadvantages, including permanent genetic changes within p53 (Lehman*, et al.*, 1993, Spanos*, et al.*, 2008b) and pRb (Kiyono*, et al.*, 1998) pathways, and isochromosomes (Allen-Hoffmann*, et al.*, 2000) that can lead to phenotypic differences compared to that of original primary cells from which they were derived. To avoid these limitations, recent research has focused on increasing cell longevity via the addition of Rho kinase inhibitors to the culture medium.

Rho-associated coiled-coiled protein kinase (ROCK) is a serine/threonine kinase important in the regulation of keratinocyte adhesion, migration and differentiation (Jackson*, et al.*, 2011, Lock and Hotchin, 2009, Narumiya*, et al.*, 1997, Tu*, et al.*, 2011) that can be inhibited through the small molecule inhibitor Y-27632 Skin, cervical and vaginal keratinocytes cultured in the presence of Y-27632 displayed an enhanced proliferative capacity and maintained an undifferentiated phenotype in monolayer culture (Chapman*, et al.*, 2010, Chapman*, et al.*, 2014, Strudwick*, et al.*, 2015). Previously, tissue engineered human skin equivalents have been cultured from Y-27632-treated dermal keratinocytes (Aslanova*, et al.*, 2015, Strudwick*, et al.*, 2015, van den Bogaard*, et al.*, 2012). However, this method has not yet been demonstrated for tonsil keratinocytes.

In this study we describe, for the first time, the generation of tissue-engineered tonsil epithelial equivalents based on Y-27632-treated tonsil keratinocytes cultured on a tonsillar fibroblast-populated de-cellularised dermis. We show that these epithelial equivalents display a structural histology and expression of epithelial markers that are

characteristic of native stratified squamous tonsil epithelium. Moreover, the *in vitro* cultured tissue demonstrates an appropriate cytokine response to infection with *S. pyogenes* and therefore represents an advanced tissue model for use in host-pathogen research.

2 Materials and Methods

All reagents were purchased from Sigma-Aldrich (Poole, UK) unless otherwise stated.

2.1 Isolation of primary human tonsillar keratinocytes and fibroblasts

All human tissues were collected from patients during routine tonsillectomies at the Royal Hallamshire Hospital, Sheffield Teaching Hospitals NHS Foundation Trust with written, informed consent (ethical approval number 09/H1308/66). Human palatine tonsils were surgically removed (Supplementary Fig. 1), placed in DMEM supplemented with 100 IU/ml penicillin, 100 µg/ml streptomycin and 0.625 µg/ml amphotericin B and transported to the laboratory. A small sample of tonsil was removed for histology before the connective tissue layer was removed and each tonsil was bisected. Enzymatic digestion of the epithelium was performed by placing each tissue half either in 0.25% w/v Difco trypsin solution or 2.5 mg/ml dispase II and the tissue was incubated overnight at 4°C. Normal tonsillar keratinocytes (NTK) were isolated by gently scraping the surface of the epithelium and crypts with a scalpel, and passed through 40µm cell sieve (Corning, New York, USA). Cells were then cultured on irradiated mouse 3T3 feeder layers in flavin- and adenine-enriched medium consisting of Dulbecco's Modified Eagle's Medium (DMEM) and Ham's F12 medium in a 3:1 (v/v) ratio supplemented with 10% (v/v) fetal

calf serum (FCS), 0.1 mM cholera toxin, 10 ng/ml epidermal growth factor (EGF), 4 µg/ml hydrocortisone, 0.025 µg/ml adenine, 5 µg/ml insulin, 5 µg/ml transferrin, 2 mM glutamine, 2 nM triiodothyronine, 0.625 µg/ml amphotericin B, 100 IU/ml penicillin and 100 µg/ml streptomycin as previously described (Allen-Hoffmann and Rheinwald, 1984). Normal tonsillar fibroblasts (NTF) were isolated from the connective tissue by fine mincing followed by digestion with either 0.5% (w/v) collagenase A overnight at 37°C or 0.5% (w/v) collagenase A overnight at 37 °C followed by trypsin-EDTA for 30 minutes at 37°C. NTF were used between passages 3 and 6 for all experiments.

2.2 Cell culture and Population doubling

NTK and the HPV oncoprotein-immortalized cell line HTE E6/E7 (provided by Prof. Eric Blair, University of Leeds, UK) were cultured in flavin- and adenine-enriched medium and NTF cultured in DMEM supplemented with 10% FCS, 2 mM glutamine, 100 IU/ml penicillin and 100 µg/ml streptomycin. All cells were cultured at 37°C, 5% CO_2 in a humidified incubator. For Rho kinase inhibition, monolayer cell cultures were incubated with flavin- and adenine-enriched medium containing 10 µg/ml of Y-27632 (Abcam, Cambridgeshire, UK) and the medium replenished every 3 days. NTK in the absence or presence of Y-27632 or HTE E6/E7 were seeded at a density of 8 x 10^3 cells per cm^2 and cultured to 80-90% confluence. Cells were then trypsinised, counted and the cell doubling time calculated using the following equation:

$$\text{Doubling time} = \frac{\text{duration of culture} \times \log(2)}{\log(\text{final cell concentration}) - \log(\text{initial cell concentration})}$$

2.3 Production of tissue-engineered tonsil epithelium equivalents

Human cadaveric skin was washed repeatedly in warm PBS and de-cellularised using 1 M sodium chloride for 24 h at 37 °C. The epithelium was removed by scraping with forceps and the connective tissue washed extensively in PBS to produce de-epidermised dermis (DED), a scaffold previously demonstrated to be ideally suited for the production of epithelium equivalents (Colley*, et al.*, 2011, MacNeil*, et al.*, 2011, Wolf*, et al.*, 2009). Twenty mm^2 pieces of DED were transferred to six-well plates (papillary surface uppermost). Tissue-engineered tonsil equivalents were produced by directly seeding 5 x 10^5 NTK and 3.3 x 10^5 NTF to the papillary surface of DED in the centre of an 8 mm diameter stainless steel ring in 450 µl of flavin- and adenine-enriched media and cells allowed to adhere in submerged culture (Fig. 1). Media inside the ring was changed after 24 h and after 72 h the ring was removed and the models placed onto stainless steel grids to facilitate culture at an air-to-liquid interface. Tonsil equivalents were cultured for 14 days before analysis, with the medium changed every 2–3 days as previously described (Colley*, et al.*, 2011).

2.4 Streptococcus pyogenes infection model

Streptococcus pyogenes leukotoxic strain C203S (Sullivan and Mandell, 1980) was routinely grown at 37°C under anaerobic conditions (10% CO_2, 10% H_2, 80% N_2) on blood agar plates made from fastidious anaerobic agar (Lab M, Heywood, UK) supplemented with 4.5% oxalated horse blood or in brain heart infusion broth supplemented with 0.5% yeast extract, 0.25% hemin, 0.1% vitamin K and 0.002% cysteine. To prepare infection models, tissue engineered tonsil equivalents were prepared as described previously, but

in these models NTF and NTK were added to 10 mm diameter discs of DED placed onto 0.4 µm pore polycarbonate transwell inserts (Millipore). Inserts were suspended on custom-made 3D printed tripod stands and cultured in 6-well plates at an air-liquid interface for 19 days, with medium changes every 2-3 days. Prior to incubation with bacteria, tonsil equivalents were cultured in antibiotic, anti-fungal and hydrocortisone-free flavin- and adenine-enriched medium overnight. *S. pyogenes* grown in liquid culture overnight at 37°C were centrifuged, washed with PBS, counted and re-suspended at 3 x 10^9 CFU/ml in antibiotic-free medium. A suspension containing 1.5 x 10^8 CFU *S. pyogenes* (multiplicity of infection = 50) was seeded onto each model and then cultured for 24 h. Non-infected models were used as controls.

2.5 Histological processing and immunohistochemistry

For histological analysis, models were removed from the culture medium, washed with PBS and fixed in 3.7% PBS-buffered formalin overnight before being subjected to routine histological processing and embedded in paraffin-wax. Five µm sections were cut using a Leica RM2235 microtome (Leica microsystems) and sections were de-waxed, rehydrated and stained with haematoxylin and eosin (H&E). For infection studies, Gram staining was used for the detection of bacteria on histology sections. For immunohistochemistry, endogenous peroxidase was neutralised with 3% hydrogen peroxide for 20 minutes. Following high-temperature citrate buffer (pH6) antigen retrieval in a 2100 Antigen Retriever (Aptum Biologics Ltd, UK), sections were blocked using protein-free blocking solution (Dako, Copenhagen, Denmark) for 20 minutes at room temperature and monoclonal primary antibodies specific to cytokeratin 8 (0.67

µg/ml, ThermoFischer Scientific), cytokeratin 13 (2.3 µg/ml, ThermoFischer Scientific), cytokeratin 14 (0.25 µg/ml, ThermoFischer Scientific), Ki67 (3 µg/ml Dako), E-cadherin (0.5 µg/ml, Abcam) or IgG isotype control (0.5 µg/ml, R&D Systems) were applied for 1 hour at room temperature. Secondary antibody and avidin-biotin complex (ABC) provided with Vectastain Elite ABC kit (Vector Labs, Peterborough, UK) were used in accordance with the manufacturer's instructions. Finally, 30-diaminobenzidine tetrahydrochloride (DAB) (Vector Labs) was used to visualise peroxidase activity and sections counterstained with haematoxylin, dehydrated and mounted in DPX. Images were taken using an Olympus BX51 microscope and Colour view IIIu camera with associated Cell^D software (Olympus Soft Imaging Solutions, Münster, Germany).

2.6 Immunoblotting

Cell pellets were washed twice with PBS and protein extracted using RIPA lysis buffer containing Halt Protease and Phosphatase Inhibitor Cocktail (ThermoFischer Scientific). Cell suspensions were vortexed, lysed using a syringe, incubated on ice for 20 minutes then centrifuged at 16 000 x g for 15 minutes at 4°C. Protein concentrations were measured using the Bicinchoninic Acid Protein Assay (ThermoFischer Scientific). Total protein extracts (30 µg) were separated using NuPAGE® 4-12% Bis-Tris SDS-PAGE gels (Life Technologies) and transferred to nitrocellulose membrane using an iBlot gel transfer device (Life Technologies). Following blocking of non-specific protein binding in 5% (w/v) dried milk, 3% (w/v) BSA in Tris-buffered saline containing 0.05% (v/v) Tween-20 (TBST) for 1 hour, membranes were incubated with monoclonal rabbit anti-p16INK4A (1:250, Sigma-Aldrich), monoclonal rabbit anti-c-MYC (1:100, Santa Cruz) or polyclonal

goat anti-β-actin (1:500; Santa Cruz) overnight at 4°C. Following washing in TBST, membranes were incubated for 2 hours with either IRDye 800CW donkey anti-rabbit (1:10 000 LI-COR Biosciences) or IRDye 680RD donkey anti-goat (1:10 000 LI-COR Biosciences). Visualization of blots and densitometry was performed using a LI-COR Odyssey system (LI-COR Biosciences).

2.7 Cytokine array

The conditioned media from *S. pyogenes*-infected and control tonsil equivalents were analysed for cytokine content using Human Cytokine Antibody Array C3 (RayBiotech, Norcross, GA) in accordance with the manufacturer's instructions. Briefly, array membranes were blocked in blocking buffer then incubated with 1 ml conditioned medium from infected or non-infected models for 2 hours at room temperature. After washing, membranes were incubated with a cocktail of biotinylated secondary antibodies for 2 hours at room temperature and then membranes washed and further incubated with horseradish peroxidase (HRP)-conjugated streptavidin followed by enhanced chemiluminescence detection. Densitometry of individual spots was undertaken using QuantityOne 4.5.0 software (BioRad) and signal intensities of cytokine spots normalised relative to internal positive and negative controls, after which relative fold change in protein level was calculated for infected compared to non-infected controls.

2.8 Lactate dehydrogenase release assay

Cell damage was analysed by measuring the release of lactate dehydrogenase (LDH) into the culture medium using a CytoTox96 enzyme assay kit (Promega, Southampton, UK) as described in the manufacturer's instructions. Briefly, 50 µl of conditioned culture medium from cell cultures was added to 50 µl of reconstituted substrate mix in a well of a 96-well flat-bottomed plate. The plate was incubated for 30 minutes at room temperature before the reaction was stopped using 50 µl acetic acid and absorbance measured at 492 nm.

2.9 Statistical analysis

Data are presented as mean values ± standard deviation (SD) of three independent experiments (n=3) with each test performed in triplicate unless otherwise stated. Mann-Whitney U tests for pairwise comparisons or ANOVA multiple statistical comparisons were performed using GraphPad Prism v6.00 (GraphPad Software, La Jolla, CA, USA) and differences between test and control groups considered significant when $p < 0.05$. Unless otherwise stated each experiment was performed on keratinocytes isolated from at least 3 different donors.

3 Results

3.1 Normal tonsillar keratinocyte and fibroblast isolation and culture

Tonsils retrieved during routine tonsillectomy were orientated to expose the oropharyngeal surface through the identification of tonsillar crypts, and the superficial stratified squamous epithelium along with the underlying connective tissue removed by scalpel excision (Supplementary Fig. 1). Enzymatic digestion of the excised tissue using trypsin yielded significantly ($p<0.05$) more NTK compared to dispase treatment, and significantly more ($p<0.05$) NTF were liberated following combined collagenase and trypsin treatment than tissue incubated with collagenase alone (Supplementary Fig. 2). Cell isolation procedures based on trypsin (NTK) and collagenase + trypsin (NTF) were therefore used throughout the study.

3.2 Rho kinase inhibition increases the longevity of normal tonsillar keratinocytes

To investigate the long-term effects of Rho kinase inhibition on proliferation and differentiation, freshly isolated NTK were cultured in the absence or presence of Y-27632. In the absence of Y-27632, NTK at low population doubling displayed a homogeneous rounded morphology with a classical cobblestone appearance (Fig. 2A). However, after prolonged culture (population doubling 11), NTK developed a flat, heterogeneous morphology with increased cell size and granulated cytoplasm reminiscent of a differentiated/senescent phenotype (Fig. 2B). Additionally, these NTK failed to proliferate beyond 13 population doublings with replicative senescence

reached at 6.3 ± 6.0 population doublings (Fig. 2E). In the presence of Y-27632, NTK at low population doubling exhibited the same classical cobblestone appearance as NTK cultured without the inhibitor (Fig. 2C). Y-27632-cultured NTK were able to proliferate in monolayer culture for approximately 70 days without loss of the cobblestone morphology or viability, reaching more than 30 population doublings before the onset of senescence (Fig. 2D & E). In contrast to NTK, HTE E6/E7 transformed keratinocytes proliferated exponentially, reaching 45 population doublings over 80 days (Fig. 2E).

3.3 Expression of p16-INK4A and C-MYC in NTK following treatment with Y27632

Altered expression of the cell cycle regulators p16-INK4A and c-MYC has previously been shown in cells upon treatment with Y-27632 (Chapman*, et al.*, 2010). Expression of p16-INK4A protein upon culture with Y-27632 was variable depending on NTK donor, with some NTK displaying reduced expression with increased population doublings (Fig 3A) whilst other isolated NTK expressed similar levels to the same NTK cultured in the absence of the inhibitor. Overall, expression of p16-INK4A was not significantly altered in NTK cultured in the presence or absence of Y-27632 at any time point analysed when examined by immunoblotting. Inn comparison, HTE E6/E7 cells displayed constitutively greater expression of p16-INK4A compared to the primary cells (Fig. 3B). Expression of c-MYC was significantly increased ($p<0.05$) in NTK cultured in Y-27632 at population doubling seven compared to cells cultured without Y-27632 (Fig. 3C). Expression of c-MYC in E6/E7 transformed HTE E6/E7 cells was significantly ($p<0.01$) greater than in NTK cultured with or without Y-27632 (Fig. 3A&C).

3.4 Generation of tissue engineered tonsil epithelium equivalents

Tissue-engineered tonsil equivalents were generated from monolayer-cultured NTK in the absence (at population doubling 3) or presence (population doubling 31) of Y-27632. NTK were added to the top of a NTF-populated DED scaffold and cultured with Y-27632-free medium at an air-to-liquid interface, and the morphology and expression of epithelial markers compared to histological sections of native tonsillar tissue. Tonsil epithelium equivalents generated from NTK cultured with or without Y-27632 both displayed a multi-layered, stratified squamous non-keratinised epithelium comprised of undifferentiated basal cells with increasingly differentiated cells toward the apical surface of the epithelium. Both tonsil epithelium equivalents were histologically similar to native human tonsillar epithelium although the epithelium in the equivalent models was thinner than observed in the native tissue (Fig. 4). In contrast, 3D equivalents generated using HTE E6/E7 cells produced models comprised of a discontinuous epithelium, often only one cell layer in thickness with a highly disorganised histological architecture (Supplementary Fig. 3). Similar to native tonsil epithelium, ki67-positive proliferating cells were confined to the basal and supra-basal layers (Fig. 4). The epithelium in both tissue equivalents was immuno-positive for E-cadherin, indicating the presence of desmosomal cell-to-cell contacts, similar to that observed in the native tonsillar epithelium (Fig. 4). Both unexposed and Y-27632-exposed tonsil epithelium equivalents were negative for cytokeratin-8 expression, as was the surface epithelium of the native tonsillar tissue. Expression of cytokeratin-13 was restricted to the upper

stratum spinosum keratinocytes in both native tonsillar epithelium and in both tissue-engineered models, and cytokeratin-14 was expressed throughout the entire epithelium in native human tissue and tonsil equivalents, although overall expression was weaker than that observed in the native epithelium (Fig. 4).

3.5 Tissue engineered tonsil epithelium equivalents based on Y-27632-treated NTK respond to S. pyogenes infection by secreting pro-inflammatory cytokines.

Tonsil epithelium equivalents were incubated for 24 hours with 1.5 x 10^8 CFU *S. pyogenes* and cytokine responses measured in order to model Group B *Streptococcus* tonsillitis. *S. pyogenes* was observed to be associated with the upper stratum spinosum layers of the epithelium only, with evidence of epithelial invasion into these keratinocytes when infected tissue sections were analysed by Gram-staining (Fig. 5). Bacterial invasion did not extend into the basal layer or the connective tissue in any of the models analysed. The culture medium from uninfected, control equivalents displayed constitutive expression of a number of cytokines including IL-6, CXCL chemokines (CXCL1-3, CXCL8, CXCL5) and CCL chemokines (CCL2, CCL8, CCL17). However, expression of many of these chemokines was significantly increased upon infection with *S. pyogenes*. For instance, expression of CXCL5 and IL-6 was increased 10-fold in infected, compared to control tonsillar epithelium equivalents (Fig. 6B). Increased expression of CCL8, EGF and OSM (approx. 4-fold increase) and the chemokines CXCL1-3, CXCL8, CCL2 and CCL17 (2-fold increase) were detected by cytokine array (Fig 6B). To confirm these findings expression of IL-6 was quantified by ELISA, which demonstrated

a significant (p=0.029) increase in IL-6 production from 2 694±760 pg/ml to 7 220±2563 pg/ml upon *S. pyogenes* infection (Fig. 6C). There was no significant difference in the viability of *S. pyogenes*-infected tonsillar epithelium equivalents compared to uninfected controls (p=0.16) (Fig. 6D).

4 Discussion

In this study we have successfully demonstrated the use the ROCK inhibitor Y-27632 to chemically increase longevity of human NTK. Similar to experiments performed using keratinocytes from other anatomical sites (dermal foreskin, cervical, vaginal; (Chapman*, et al.*, 2014, Strudwick*, et al.*, 2015)), we observed prolonged cell doubling time in culture, with NTK reaching up to 31 population doublings without loss of morphology or replicative senescence. In contrast, NTK cultured in the absence of ROCK inhibitor quickly succumbed to replicative senescence and terminated proliferation. Like with other keratinocytes, the ability to extend the life span of NTK using Y-27632 without altering their phenotype has great implications for the use of these cells in research.

It is known that alterations in the expression of key cell cycle regulating proteins such as c-MYC and p16INK4A are crucial for cell immortalisation (Liu*, et al.*, 2008). The transcription factor c-MYC binds to human telomerase reverse transcriptase (hTERT) - the catalytic subunit of telomerase - to induce its transcription and elevated levels of this enzyme are associated with increased telomere lengths and extended cell longevity (Liu*, et al.*, 2008). We found that c-MYC protein levels in NTK significantly increased upon addition of Y-27632 to the culture medium, suggesting that elevated levels of c-MYC

expression may, in part, be responsible for driving ROCK inhibitor-induced increase in lifespan. Similar observations have been reported for dermal keratinocytes, where Y-27632 also rapidly induced c-MYC expression (Chapman*, et al.*, 2010).

Increased telomerase expression alone is not enough to sufficiently immortalise keratinocytes and expression of other cell cycle regulators such as p16INK4A must also be down-regulated (Dickson*, et al.*, 2000, Kiyono*, et al.*, 1998). On this basis, p16INK4A expression was examined in NTK grown in the presence and absence of Y-27632. Similar to observations for Y-27632-treated dermal, vaginal and cervical keratinocytes, we observed variable expression of p16INK4A for NTK in the presence of the ROCK inhibitor over several population doublings, a finding that was donor dependent (Chapman*, et al.*, 2010). Although further experimentation is required, our data support the notion that Y-27632 alters the expression of key cell cycle regulating proteins, in particular c-MYC, to impart an increased proliferation capacity on NTK. In HPV E6/E7 immortalized cells expression of p16INK4A was markedly elevated, even so, this protein is ineffectual due to inactivation of the pRb retinoblastoma tumour suppressor pathway by E7 (Kiyono*, et al.*, 1998).

To our knowledge, this is the first study that describes the use of Y-27632-treated NTK along with autologous NTF to produce a full-thickness tonsillar tissue. Chapman *et al* demonstrated that Y-27632 inhibits keratinocyte differentiation whilst promoting proliferation (Chapman*, et al.*, 2014), although this increase in lifespan could be reversed upon withdrawal of inhibitor. Therefore, Y-27632 was removed from NTK monolayers before adding these cells to the NTF-populated dermis, enabling the cells to

produce a stratified, differentiated epithelium. Tonsil epithelium equivalents generated from NTK cultured in the presence of Y-27632 displayed the same histological appearance and expressed proliferation and differentiation markers that were directly comparable to normal human tonsil tissue, even after prolonged monolayer culture at a population doubling of 31; a period where NTK cultured in the absence of the inhibitor had already undergone senescence. In addition, tonsil equivalents based on Y-27632-cultured NTK had the same morphology and characteristics as equivalents made with NTK cultured without the inhibitor (Temple*, et al.*, 2014). Use of Y-27632 greatly expands the window of opportunity to use cells for tissue engineering, allowing large numbers of replicate tonsil equivalents to be produced over an extended period of population doublings, an obvious advantage for *in vitro* experimentation.

Tonsil equivalents generated from NTK grown in the absence or presence of Y-27632 failed to express cytokeratin-8, a specific marker for tonsil crypt keratinocytes (Clark*, et al.*, 2000), suggesting that the treated NTK are derived from the surface tonsil epithelium. Both epithelial equivalents displayed ki-67-positive immune-positive cells in the basal layer representing actively proliferating cells within the stratified epithelium. Evidence suggests that HPV preferentially infects the basal cells of oropharyngeal squamous epithelium to establish long-term infection. Here, the viral plasmid is retained within the basal cells in low copy number, but as the keratinocytes differentiate towards the apical surface the HPV plasmid levels increase rapidly and viral-laden keratinocytes cells are finally shed from the epithelial surface. Integration of HPV plasmid into the basal cell host DNA can also occur and this is associated with carcinogenesis (Doorbar, 2016, Doorbar*, et al.*, 2015). Therefore, examining HPV biology in its natural

environment necessitates the use of a proliferating stratified epithelium. The ability to create reproducible, fully-differentiated *in vitro* models of tonsillar epithelium has the potential to dramatically expedite research into oropharyngeal HPV infection, persistence and carcinogenesis; experiments that have previously required access to freshly isolated tissue.

We further validated the functionality of our tonsil epithelium equivalent by performing infection studies with *S. pyogenes*, the organism most often associated with bacterial tonsillitis. Tonsil infection is associated with recruitment of innate immune cells mediated by release of chemokines from locally infected cells (Rudack*, et al.*, 2004). Persson *et al* showed that *S. pyogenes* initiates a pro-inflammatory response from monolayer-cultured keratinocytes in a Toll-Like Receptor-dependent mechanism by releasing chemokines such as CXCL1 and CXCL8 (Persson*, et al.*, 2015). We observed a similar pattern of pro-inflammatory cytokine production in tonsil epithelium equivalents infected with *S. pyogenes* where cytokine array profiling detected marked increases in several pro-inflammatory chemokines aimed at neutrophil (CXCL1, CXCL8) and mononuclear leukocyte (CCL2, CCL5) recruitment. In addition, and unlike previous studies, we detected a significant increase in IL-6 secretion, a cytokine highly expressed by fibroblasts during infection (Into*, et al.*, 2010); data that underscores the importance of performing infection studies using co-cultured cells set in a more natural environment. Recent evidence suggests that a dramatic genomic shift has occurred in a particular strain of Group A *Streptococcus* (genotype emm89) causing this bacterium to obtain molecular features that increase its virulence, which has led to epidemic waves of infection worldwide (Turner*, et al.*, 2015). Defining the molecular interaction between

emm89 and the tonsillar epithelium would greatly enhance our knowledge of the new pathogenic mechanisms initiated by this bacterial strain, and studies utilising 3D, stratified squamous epithelium that closely mimics normal tonsillar epithelium will be crucial in unravelling the disease process.

In summary, we have shown that Y-27632 is able to increase the longevity of tonsillar keratinocytes and that these cells can be used to produce biologically functional tissue engineered tonsillar epithelium equivalents that closely mimic the natural human tissue. The increased availability of such models has significant implications for those researchers studying the pathogenesis of HPV, EBV and Group A *Streptococcus* infection, where tissue structure and architecture is of paramount importance.

5 Acknowledgements

The authors would like to thank Jason Heath for microbiological technical support and Jordan Lee for assistance with NTF isolation.

6 References

Abbot EL, Smith WD, Siou GP*, et al.* 2007, Pili mediate specific adhesion of Streptococcus pyogenes to human tonsil and skin, *Cellular microbiology*, **9** (7): 1822-1833.

Ajello M, Greco R, Giansanti F*, et al.* 2002, Anti-invasive activity of bovine lactoferrin towards group A streptococci, *Biochem Cell Biol*, **80** (1): 119-124.

Allen-Hoffmann BL, Rheinwald JG. 1984, Polycyclic aromatic hydrocarbon mutagenesis of human epidermal keratinocytes in culture, *Proceedings of the National Academy of Sciences of the United States of America*, **81** (24): 7802-7806.

Allen-Hoffmann BL, Schlosser SJ, Ivarie CA*, et al.* 2000, Normal growth and differentiation in a spontaneously immortalized near-diploid human keratinocyte cell line, NIKS, *The Journal of investigative dermatology*, **114** (3): 444-455.

Aslanova A, Takagi R, Yamato M*, et al.* 2015, A chemically defined culture medium containing Rho kinase inhibitor Y-27632 for the fabrication of stratified squamous epithelial cell grafts, *Biochemical and biophysical research communications*, **460** (2): 123-129.

Bell S, Howard A, Wilson JA*, et al.* 2012, Streptococcus pyogenes infection of tonsil explants is associated with a human beta-defensin 1 response from control but not recurrent acute tonsillitis patients, *Molecular oral microbiology*, **27** (3): 160-171.

Chapman S, Liu X, Meyers C*, et al.* 2010, Human keratinocytes are efficiently immortalized by a Rho kinase inhibitor, *The Journal of clinical investigation*, **120** (7): 2619-2626.

Chapman S, McDermott DH, Shen K*, et al.* 2014, The effect of Rho kinase inhibition on long-term keratinocyte proliferation is rapid and conditional, *Stem Cell Res Ther*, **5** (2): 60.

Clark MA, Wilson C, Sama A*, et al.* 2000, Differential cytokeratin and glycoconjugate expression by the surface and crypt epithelia of human palatine tonsils, *Histochem Cell Biol*, **114** (4): 311-321.

Colley HE, Hearnden V, Jones AV*, et al.* 2011, Development of tissue-engineered models of oral dysplasia and early invasive oral squamous cell carcinoma, *British journal of cancer*, **105** (10): 1582-1592.

Dickson MA, Hahn WC, Ino Y*, et al.* 2000, Human keratinocytes that express hTERT and also bypass a p16(INK4a)-enforced mechanism that limits life span become immortal yet retain normal growth and differentiation characteristics, *Molecular and cellular biology*, **20** (4): 1436-1447.

Doorbar J. 2016, Model systems of human papillomavirus-associated disease, *J Pathol*, **238** (2): 166-179.

Doorbar J, Egawa N, Griffin H*, et al.* 2015, Human papillomavirus molecular biology and disease association, *Rev Med Virol*, **25 Suppl 1**: 2-23.

Into T, Inomata M, Shibata K*, et al.* 2010, Effect of the antimicrobial peptide LL-37 on Toll-like receptors 2-, 3- and 4-triggered expression of IL-6, IL-8 and CXCL10 in human gingival fibroblasts, *Cell Immunol*, **264** (1): 104-109.

Ishizaki T, Uehata M, Tamechika I*, et al.* 2000, Pharmacological properties of Y-27632, a specific inhibitor of rho-associated kinases, *Mol Pharmacol*, **57** (5): 976-983.

Jackson B, Peyrollier K, Pedersen E*, et al.* 2011, RhoA is dispensable for skin development, but crucial for contraction and directed migration of keratinocytes, *Mol Biol Cell*, **22** (5): 593-605.

Kang SY, Kannan N, Zhang L*, et al.* 2015, Characterization of Epithelial Progenitors in Normal Human Palatine Tonsils and Their HPV16 E6/E7-Induced Perturbation, *Stem cell reports*, **5** (6): 1210-1225.

Kiyono T, Foster SA, Koop JI*, et al.* 1998, Both Rb/p16INK4a inactivation and telomerase activity are required to immortalize human epithelial cells, *Nature*, **396** (6706): 84-88.

Lace MJ, Anson JR, Klingelhutz AJ*, et al.* 2009a, Human papillomavirus (HPV) type 18 induces extended growth in primary human cervical, tonsillar, or foreskin keratinocytes more effectively than other high-risk mucosal HPVs, *Journal of virology*, **83** (22): 11784-11794.

Lace MJ, Isacson C, Anson JR*, et al.* 2009b, Upstream regulatory region alterations found in human papillomavirus type 16 (HPV-16) isolates from cervical carcinomas increase transcription, ori function, and HPV immortalization capacity in culture, *Journal of virology*, **83** (15): 7457-7466.

Lehman TA, Modali R, Boukamp P*, et al.* 1993, p53 mutations in human immortalized epithelial cell lines, *Carcinogenesis*, **14** (5): 833-839.

Liu X, Dakic A, Chen R*, et al.* 2008, Cell-restricted immortalization by human papillomavirus correlates with telomerase activation and engagement of the hTERT promoter by Myc, *Journal of virology*, **82** (23): 11568-11576.

Lock FE, Hotchin NA. 2009, Distinct roles for ROCK1 and ROCK2 in the regulation of keratinocyte differentiation, *PloS one*, **4** (12): e8190.

Lundberg AS, Hahn WC, Gupta P*, et al.* 2000, Genes involved in senescence and immortalization, *Current opinion in cell biology*, **12** (6): 705-709.

MacNeil S, Shepherd J, Smith L. 2011, Production of tissue-engineered skin and oral mucosa for clinical and experimental use, *Methods in molecular biology*, **695**: 129-153.

Mah W, Jiang G, Olver D*, et al.* 2014, Human gingival fibroblasts display a non-fibrotic phenotype distinct from skin fibroblasts in three-dimensional cultures, *PloS one*, **9** (3): e90715.

Moharamzadeh K, Colley H, Murdoch C*, et al.* 2012, Tissue-engineered oral mucosa, *Journal of dental research*, **91** (7): 642-650.

Narumiya S, Ishizaki T, Watanabe N. 1997, Rho effectors and reorganization of actin cytoskeleton, *FEBS Lett*, **410** (1): 68-72.

Pegtel DM, Middeldorp J, Thorley-Lawson DA. 2004, Epstein-Barr virus infection in ex vivo tonsil epithelial cell cultures of asymptomatic carriers, *Journal of virology*, **78** (22): 12613-12624.

Persson ST, Wilk L, Morgelin M*, et al.* 2015, Vigilant keratinocytes trigger pathogen-associated molecular pattern signaling in response to streptococcal M1 protein, *Infection and immunity*, **83** (12): 4673-4681.

Ramirez RD, Morales CP, Herbert BS*, et al.* 2001, Putative telomere-independent mechanisms of replicative aging reflect inadequate growth conditions, *Genes & development*, **15** (4): 398-403.

Reijnders CM, van Lier A, Roffel S*, et al.* 2015, Development of a Full-Thickness Human Skin Equivalent In Vitro Model Derived from TERT-Immortalized Keratinocytes and Fibroblasts, *Tissue Eng Part A*, **21** (17-18): 2448-2459.

Rudack C, Jorg S, Sachse F. 2004, Biologically active neutrophil chemokine pattern in tonsillitis, *Clin Exp Immunol*, **135** (3): 511-518.

Smith WD, Pointon JA, Abbot E*, et al.* 2010, Roles of minor pilin subunits Spy0125 and Spy0130 in the serotype M1 Streptococcus pyogenes strain SF370, *J Bacteriol*, **192** (18): 4651-4659.

Spanos WC, Geiger J, Anderson ME*, et al.* 2008a, Deletion of the PDZ motif of HPV16 E6 preventing immortalization and anchorage-independent growth in human tonsil epithelial cells, *Head & neck*, **30** (2): 139-147.

Spanos WC, Hoover A, Harris GF*, et al.* 2008b, The PDZ binding motif of human papillomavirus type 16 E6 induces PTPN13 loss, which allows anchorage-independent growth and synergizes with ras for invasive growth, *Journal of virology*, **82** (5): 2493-2500.

Sriram G, Bigliardi PL, Bigliardi-Qi M. 2015, Fibroblast heterogeneity and its implications for engineering organotypic skin models in vitro, *European journal of cell biology*, **94** (11): 483-512.

Strudwick XL, Lang DL, Smith LE*, et al.* 2015, Combination of low calcium with Y-27632 rock inhibitor increases the proliferative capacity, expansion potential and lifespan of primary human keratinocytes while retaining their capacity to differentiate into stratified epidermis in a 3D skin model, *PloS one*, **10** (4): e0123651.

Sullivan GW, Mandell GL. 1980, Interactions of human neutrophils with leukotoxic streptococci, *Infection and immunity*, **30** (1): 272-280.

Syrjanen S. 2004, HPV infections and tonsillar carcinoma, *Journal of clinical pathology*, **57** (5): 449-455.

Temple RM, Zhu J, Budgeon L*, et al.* 2014, Efficient replication of Epstein-Barr virus in stratified epithelium in vitro, *Proceedings of the National Academy of Sciences of the United States of America*, **111** (46): 16544-16549.

Tu CL, Chang W, Bikle DD. 2011, The calcium-sensing receptor-dependent regulation of cell-cell adhesion and keratinocyte differentiation requires Rho and filamin A, *The Journal of investigative dermatology*, **131** (5): 1119-1128.

Turner CE, Abbott J, Lamagni T*, et al.* 2015, Emergence of a New Highly Successful Acapsular Group A Streptococcus Clade of Genotype emm89 in the United Kingdom, *MBio*, **6** (4): e00622.

Turner CE, Sommerlad M, McGregor K*, et al.* 2012, Superantigenic activity of emm3 Streptococcus pyogenes is abrogated by a conserved, naturally occurring smeZ mutation, *PloS one*, **7** (10): e46376.

Uehata M, Ishizaki T, Satoh H*, et al.* 1997, Calcium sensitization of smooth muscle mediated by a Rho-associated protein kinase in hypertension, *Nature*, **389** (6654): 990-994.

van den Bogaard EH, Rodijk-Olthuis D, Jansen PA*, et al.* 2012, Rho kinase inhibitor Y-27632 prolongs the life span of adult human keratinocytes, enhances skin equivalent development, and facilitates lentiviral transduction, *Tissue Eng Part A*, **18** (17-18): 1827-1836.

Wilkening RV, Federle MJ. 2017, Evolutionary Constraints Shaping Streptococcus pyogenes-Host Interactions, *Trends Microbiol*.

Wolf K, Alexander S, Schacht V*, et al.* 2009, Collagen-based cell migration models in vitro and in vivo, *Semin Cell Dev Biol*, **20** (8): 931-941.

Yamaguchi H, Miwa Y, Kasa M*, et al.* 2006, Structural basis for induced-fit binding of Rho-kinase to the inhibitor Y-27632, *J Biochem*, **140** (3): 305-311.

7 Figure Legends

Figure 1: Schematic diagram to demonstrate method used to produce tissue engineered tonsil equivalents. DED= de-epidermised dermis, NTK= normal tonsillar keratinocytes and NTF= Normal tonsillar fibroblasts.

Figure 2: Incubation with Y-27632 maintains an undifferentiated epithelial morphology and significantly increases the number of population doublings of primary tonsillar keratinocytes in culture. Representative phase contrast images of NTK showing that the cobblestone morphology of (A) monolayer cultured early passage NTK (PD=3) and the altered morphology these cells undergo after prolonged culture (B). NTK cultured in the presence of the rho kinase inhibitor Y-27632 exhibit a typical cobblestone morphology after at both early stages of culture (PD=3, C) and after prolonged culture (PD=31, D) Scale bar= 100 µm. (E) Cell proliferation rates were determined by calculating population doubling times for normal tonsil keratinocytes (NTK) from 5 independent donors cultured in the absence (red circles) or presence (blue squares) of 10 µM Y-27632 and compared to the growth of the HPV-immortalized cell line HTE E6/E7 (black triangles).

Figure 3: Relative protein expression of p16-INK4A and c-MYC in NTK cultured in the presence or absence of Y-27632. (A) Cell lysates from monolayer NTK cultured in the absence (PD= 5) or presence of Y-27632 (PD= 7 and 22) were separated by SDS-PAGE and immunoblotting performed for expression of p16-INK4A, c-MYC and β-actin as a loading control. Expression of p16-INK4A and c-MYC in the HPV-transformed cell line

HTE E6/E7 was used as a positive control. Immunoblot band intensities were determined by densitometry and normalised to β-actin levels for (B) p16-INK4A and (C) c-MYC. Representative data from experiments performed on NTK from three independent donors.

Figure 4: Y27632-treated normal tonsil keratinocyte (NTK) with increased lifespan can be used to generate 3D tonsil epithelium equivalents that display similar characteristics to low passage untreated NTK and human tonsillar tissue. Tissue-engineered tonsil epithelium equivalents were generated by culturing Y-27632-treated normal tonsillar keratinocytes (NTK at PD=31) on top of a normal tonsillar fibroblast-populated DED scaffold and compared to equivalents prepared from low passage NTK (PD=3) in the absence of Y-27632 and normal human tonsil (NHT) tissue. Histological (haematoxylin and eosin, H&E) and immunohistochemical analysis for ki-67, E-cadherin, cytokeratin 8, 13 and 14 were used to characterise the models. Representative images are from three independent experiments. Scale bar = 50 μm.

Figure 5: 3D tissue engineered tonsil epithelium equivalents infected with *Streptococcus pyogenes* to model tonsillitis. H&E and Gram-stained images of uninfected control (A-B) and *S. pyogenes* infected (MOI 50) tissue-engineered tonsil epithelium equivalents (C-D) generated from Y-27632-treated NTK. Image in D shows Gram-positive *S. pyogenes* (blue dots) associated with the upper stratum spinosum layers of the tonsil epithelium. Scale bars = 100 (A&C) and 20 (B&D) μm respectively.

Figure 6: *Streptococcus pyogenes*-infected tonsil epithelium equivalents display increased expression of pro-inflammatory cytokines compared to untreated controls. Tissue engineered tonsil epithelium equivalents generated from Y-27632-treated NTK were incubated with *S. pyogenes* to model tonsillitis and the expression of pro-inflammatory cytokines measured by cytokine array. (A) Representative immunoblots of cytokine arrays showing levels of cytokines in the conditioned medium of uninfected controls compared to *S. pyogenes*-infected equivalents. (B) Densitometry analysis of array immunoblots showing fold change expression of cytokines in *S. pyogenes*-infected equivalents compared to controls. (C) Quantitative measurement of IL-6 by ELISA showing significant increase in expression in infected compared to uninfected control equivalents. (D) Lactate dehydrogenase release in infected compared to uninfected control equivalents. *$p<0.05$, data in A&B are from 2 independent experiments with tonsil equivalents from each experiment derived from different donors. Data in C&D are the mean ± SD from n=4 independent experiments using cells from 3 independent donors.

Supplementary figure 1: Surgical anatomy of tonsils immediately before and after excision. (A) Clinical anatomy of tonsils prior to excision. 1. Upper incisor, 2. Uvula, 3. Right tonsil, 4. Left tonsil, 5. Lower third molar tooth, 6. Tongue dorsum, 7. Fenestrated surgical retractor (tongue dorsum seen protruding through fenestration), 8. Anaesthetic tubing. (B) Oropharyngeal surface of excised tonsil prior to use in cell culture. Note that

the oropharyngeal surface can be orientated through identification of tonsillar crypts surrounded by a smooth, pale surface epithelium. Tonsillar keratinocytes were harvested from regions of surface epithelium by scalpel excision under sterile tissue culture conditions**.** (C) Deep surface of excised tonsil prior to use in cell culture. Note the haemorrhagic surface, which includes a cauterised pedicle consisting of tonsillar arterial branches and the peritonsillar venous plexus. Presence of cautery marks, in addition to a more corrugated texture, assist in distinguishing the deep surface, which is devoid of epithelium and will therefore lead to poor keratinocyte yields.

Supplementary figure 2: Efficiency of NTK and NTF isolation using different enzymatic treatments. (A) Excised tonsillar tissue was incubated with either trypsin or dispase II and NTK isolation efficacy determined by cell counting. (B) Treatment of connective tissue with collagenase alone or a mixture of collagenase/trypsin for the efficacy of NTF isolation. *$p<0.05$, data are mean ± SD from n=4 independent experiments.

Supplementary figure 3: The HPV-immortalized cell line HTE E6/E7 do not form a stratified epithelium in tissue-engineered models. Tissue-engineered models were generated by culturing HTE E6/E7 on top of a NTF-populated DED scaffold. Histological analysis by H&E staining revealed that the cells failed to form a stratified epithelium after 14 days in culture. Scale bar = 100 µm.

Figure 1

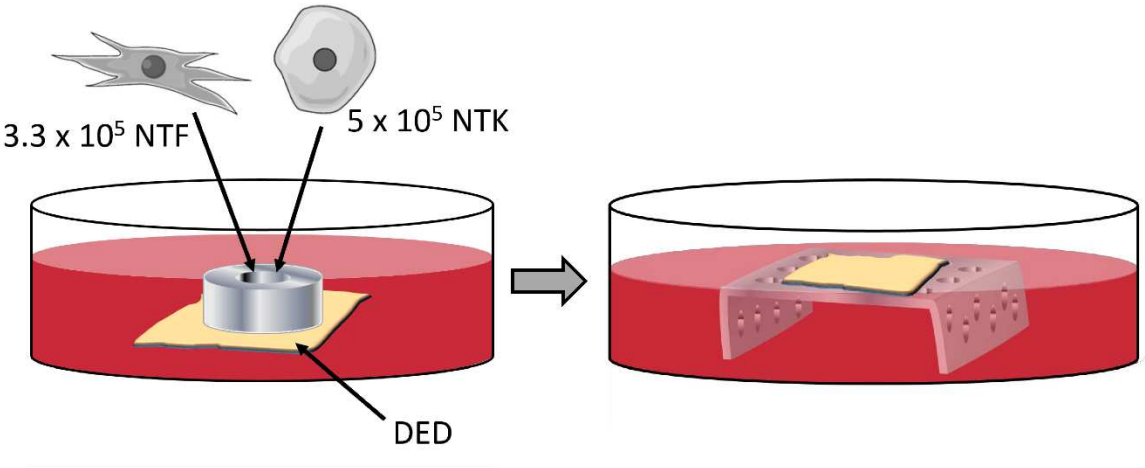

Figure 2

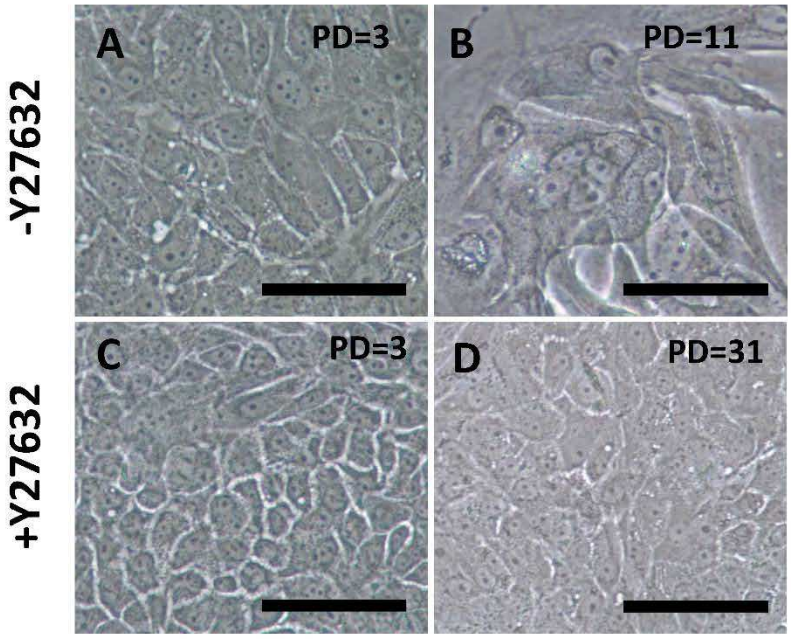
A
PD=3
B
PD=11
-Y27632
C
PD=3
D
PD=31
+Y27632

E

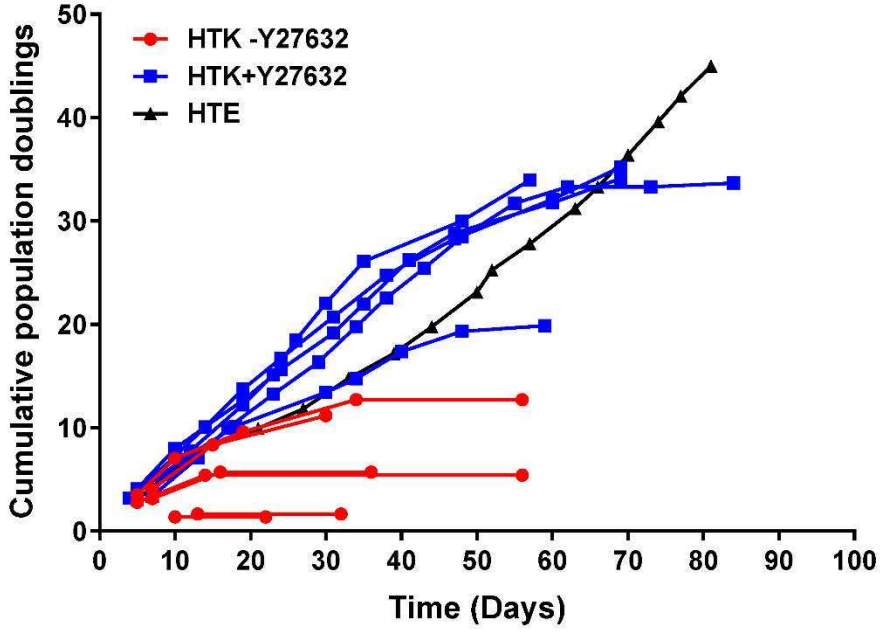
HTK -Y27632
HTK+Y27632
HTE
Cumulative population doublings
Time (Days)
0
10
20
30
40
50
60
70
80
90
100

Figure 3

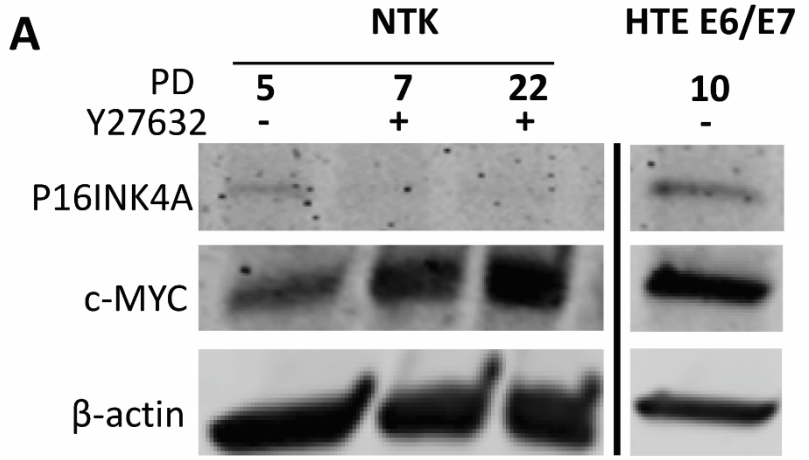
A
NTK
HTE E6/E7
PD
5
7
22
10
Y27632
-
+
+
-
P16INK4A
c-MYC
β-actin

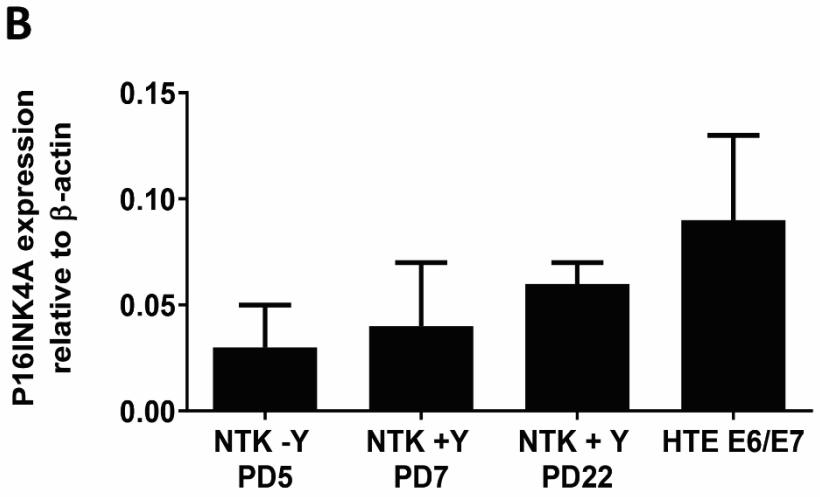
B
P16INK4A expression relative to β-actin
0.15
0.10
0.05
0.00
NTK -Y PD5
NTK +Y PD7
NTK + Y PD22
HTE E6/E7

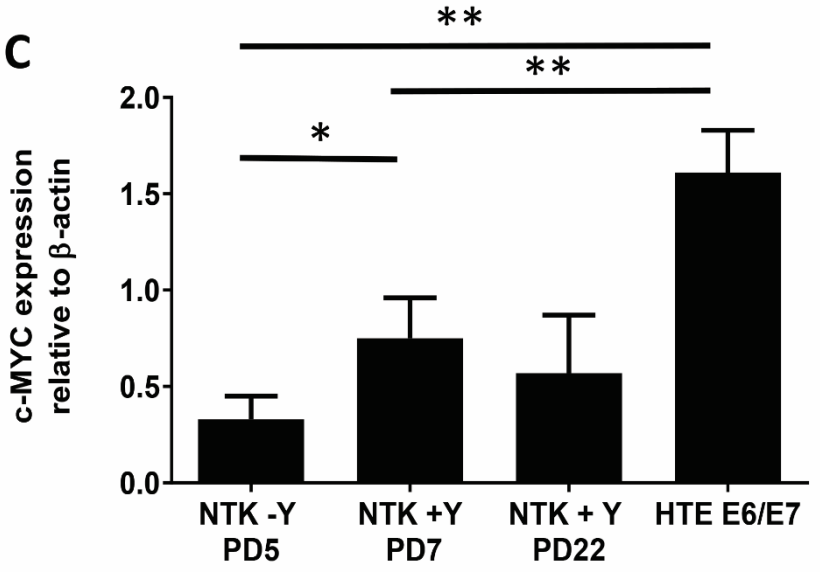
C
**
**
*
c-MYC expression relative to β-actin
2.0
1.5
1.0
0.5
0.0
NTK -Y PD5
NTK +Y PD7
NTK + Y PD22
HTE E6/E7

Figure 4

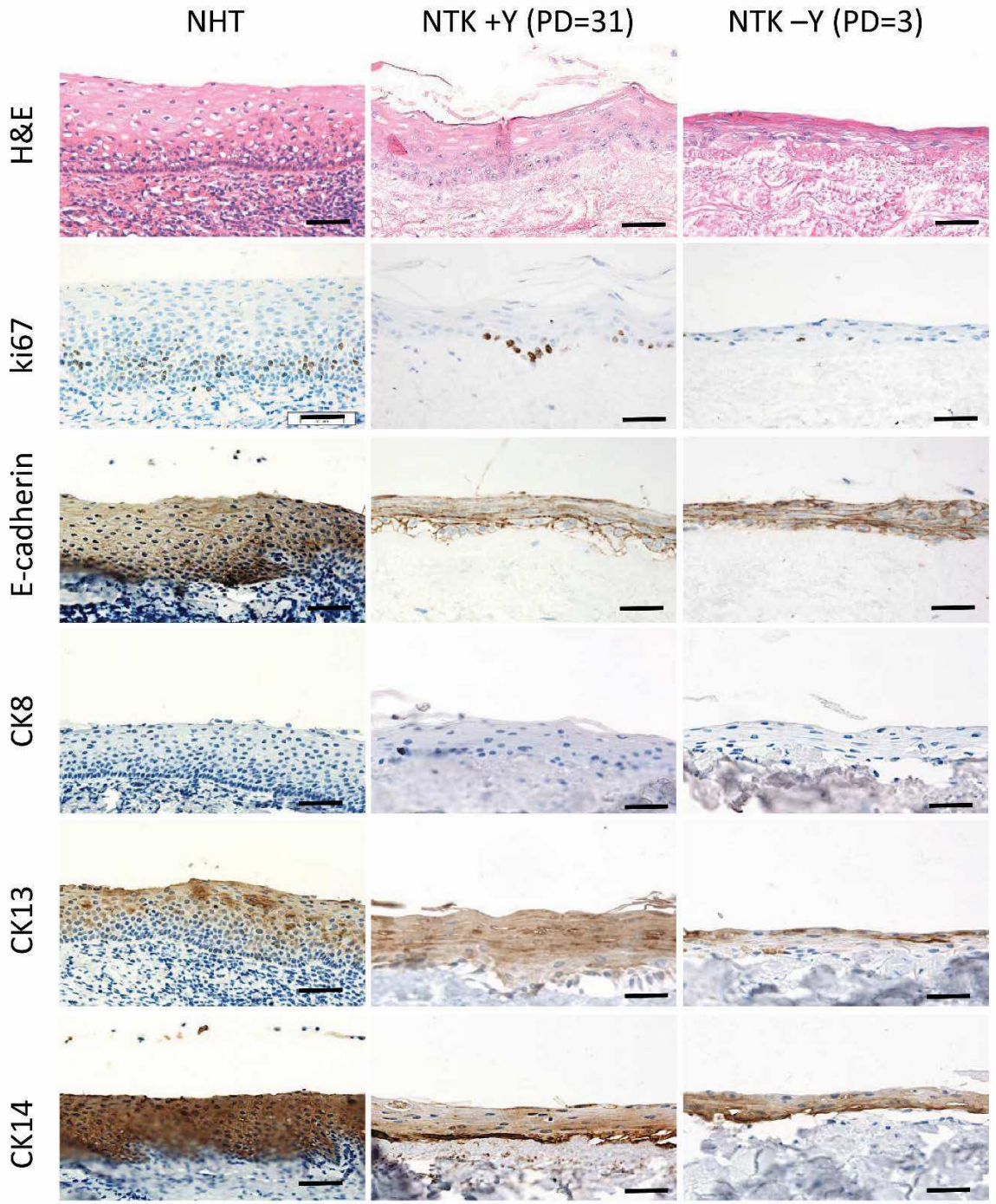

Figure 5

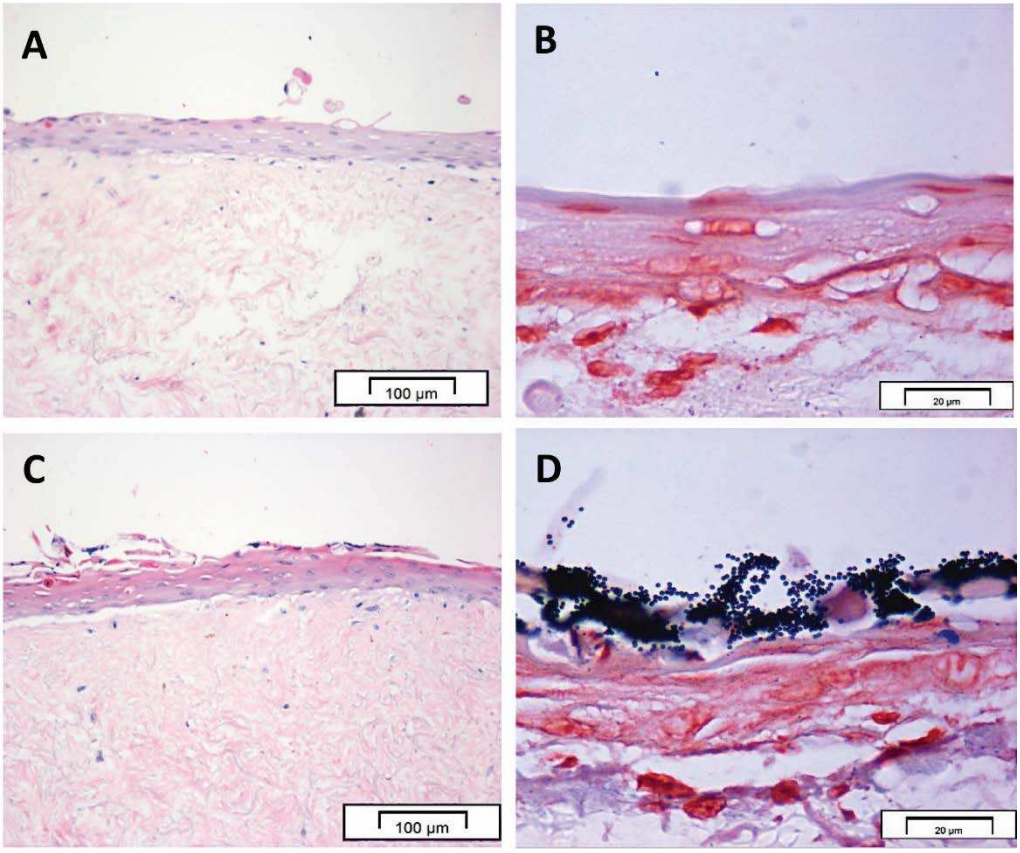

Figure 6

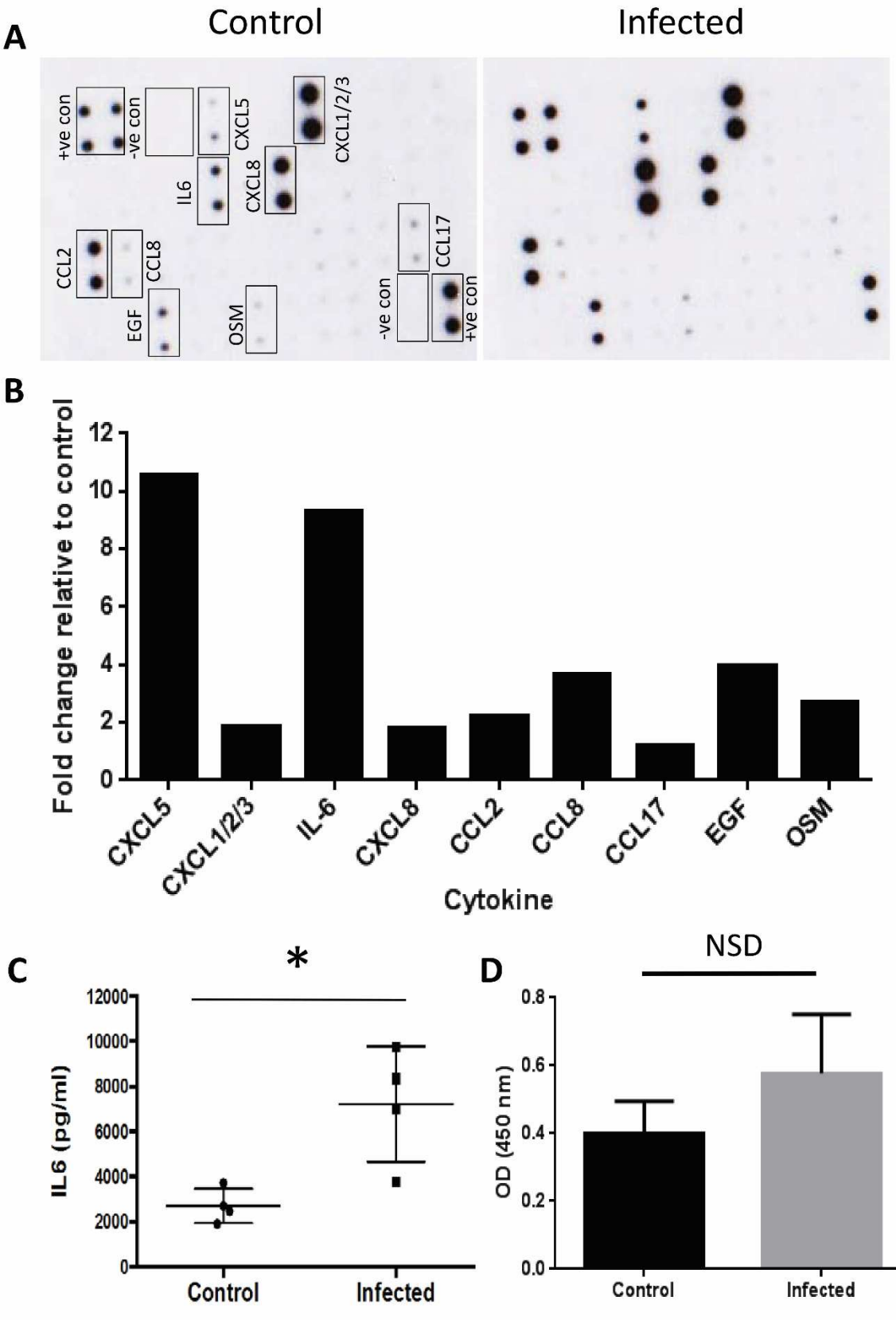
A
Control
Infected
+ve con
-ve con
CXCL5
CXCL1/2/3
IL6
CXCL8
CCL2
CCL8
EGF
OSM
CCL17
-ve con
+ve con
B
Fold change relative to control
0
2
4
6
8
10
12
CXCL5
CXCL1/2/3
IL-6
CXCL8
CCL2
CCL8
CCL17
EGF
OSM
Cytokine
C
*
IL6 (pg/ml)
0
2000
4000
6000
8000
10000
12000
Control
Infected
D
NSD
OD (450 nm)
0.0
0.2
0.4
0.6
0.8
Control
Infected